

Nonequilibrium sensing and its analogy to kinetic proofreading

David Hartich, Andre C. Barato, and Udo Seifert

II. Institut für Theoretische Physik, Universität Stuttgart, 70550 Stuttgart, Germany

E-mail: hartich@theo2.physik.uni-stuttgart.de, barato@theo2.physik.uni-stuttgart.de
and useifert@theo2.physik.uni-stuttgart.de

Abstract. For a paradigmatic model of chemotaxis, we analyze the effect of how a nonzero affinity driving receptors out of equilibrium affects sensitivity. This affinity arises whenever changes in receptor activity involve ATP hydrolysis. The sensitivity integrated over a ligand concentration range is shown to be enhanced by the affinity, providing a measure of how much energy consumption improves sensing. With this integrated sensitivity we can establish an intriguing analogy between sensing with nonequilibrium receptors and kinetic proofreading: the increase in integrated sensitivity is equivalent to the decrease of the error in kinetic proofreading. The influence of the occupancy of the receptor on the phosphorylation and dephosphorylation reaction rates is shown to be crucial for the relation between integrated sensitivity and affinity. This influence can even lead to a regime where a nonzero affinity decreases the integrated sensitivity, which corresponds to anti-proofreading.

1. Introduction

Bacterial chemotaxis, a process by which the cell directs its motion in response to external ligand concentration, is a canonical example of biological sensing. Experiments with *E. coli* have provided much insight into chemotaxis [1, 2], making this bacterium sensory system a particularly well understood example. In *E. coli* chemotaxis, the sensitivity is a key observable quantifying the response in activity inside the cell due to a change in the external ligand concentration.

Stochastic models for *E. coli* [3–6] receptors often assume that changes in activity are described by an equilibrium process involving only conformational changes, leading to an equilibrium Monod-Wyman-Changeux (MWC) model [7, 8]. However, chemical reactions where the receptor changes from an inactive to an active state often involve free energy consumption through, for example, adenosine triphosphate (ATP) hydrolysis. A stochastic model including this feature must have transition rates that break detailed balance leading to a nonzero affinity, corresponding to the chemical potential difference involved in ATP hydrolysis, driving the process out of equilibrium.

Two recent studies have analyzed the effect of such an affinity in models related to the *E. coli* sensory network. Tu [9] has considered the effect of the driving affinity on both the dwell-time distribution and the sensitivity in a model for the flagellar motor switching between run and tumble. Skoge et al. [10] have shown that nonequilibrium receptors can increase the signal to noise ratio for fixed sensitivity.

Beyond *E. coli* chemotaxis, the effect of energy dissipation in biological processes involving information processing has received much attention recently [11–21]. A prominent example among such processes is kinetic proofreading [22–25], which is a dissipative error reduction mechanism related to copying biochemical information. As this error reduction is achieved through free energy consumption, a nonzero affinity driving the process out of equilibrium is also present in kinetic proofreading. Specifically, relations between the error and the driving affinity have been obtained [25, 26] (see also [27–32] for other recent works).

In this paper, we consider a nonequilibrium model for *E. coli* receptors including ATP hydrolysis in the chemical reactions that involve changes in activity. We quantify the effect of having a nonzero driving affinity on sensing by analyzing an integrated sensitivity, which is an integral of the sensitivity over a concentration range. This observable is shown to have a simple relation with the affinity driving the process out of equilibrium. We show that sensing with nonequilibrium receptors and kinetic proofreading can be viewed as equivalent problems, with the increase in the integrated sensitivity in nonequilibrium sensing being analogous to the error reduction in kinetic proofreading.

The transition rates for changes in activity are assumed to depend on whether the receptor is occupied by a ligand or empty. We show that this dependency is quite important for the relation between sensitivity and the driving affinity. There is even a regime where energy dissipation leads to a decrease in the integrated sensitivity, which is equivalent to an anti-proofreading regime in kinetic proofreading [32].

The paper is organized as follows. Section 2 contains a simple stochastic model for a single nonequilibrium receptor. In section 3 we introduce the integrated sensitivity and obtain its relation with the affinity driving the process out of equilibrium. The analogy between nonequilibrium sensing and proofreading is established in section 4. In section 5, with a more general model for a single receptor, we analyze how the influence of the occupancy of the receptor on the phosphorylation and dephosphorylation reaction rates affects the relation between integrated sensitivity and affinity. We conclude in section 6. Moreover, Appendix A contains a generalization of the single receptor model analyzed in the main text to an arbitrary number of binding sites.

2. Nonequilibrium receptor model

The single receptor model we analyze in this paper is defined as follows (see Fig. 1). There are two binary variables a and b characterizing the state of the receptor, with $b = 1$ if the receptor is occupied by a ligand (bound) and $b = 0$ if the receptor is free

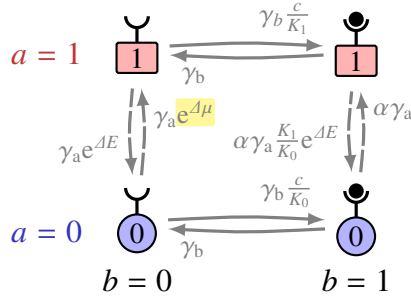


Figure 1. Four-state model for a single receptor. Vertical transitions correspond to a change in activity, while horizontal transitions correspond to a change in the occupancy of the receptor. The phosphorylation rates in (4) are chosen as $\kappa_+^0 = \gamma_b e^{\Delta\mu}$ and $\kappa_-^0 = \gamma_a e^{\Delta E}$. The dephosphorylation rates in (5) are chosen as $\omega_+ = \alpha\gamma_a (K_1/K_0)e^{\Delta E}$ and $\omega_- = \alpha\gamma_a$.

(unbound), and $a = 1$ if the receptor is active and $a = 0$ if the receptor is inactive.

In equilibrium the free energy of the four different states can be written as [8, 20]

$$F(a, b) \equiv a\Delta E - b \ln \frac{c}{K_a}, \quad (1)$$

where ΔE is the conformational energy difference between active and inactive for a free receptor ($b = 0$), K_a is the dissociation constant that depends on the activity a , and c is the external ligand concentration. Setting Boltzmann's constant and the temperature to $k_B T \equiv 1$, the equilibrium stationary probability is $P_{a,b} \propto \exp[-F(a, b)]$. Denoting the coarse-grained probability by $P_a \equiv \sum_{b'} P_{a,b'}$, we obtain

$$\left. \frac{P_0}{P_1} \right|_{\text{eq}} = e^{\Delta E} \left(\frac{1 + \frac{c}{K_0}}{1 + \frac{c}{K_1}} \right), \quad (2)$$

where $P_0 = 1 - P_1$. The average activity

$$\langle a \rangle_c \equiv \sum_a a P_a \quad (3)$$

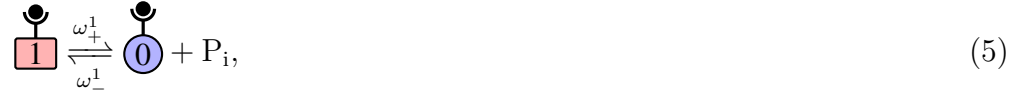
is just $\langle a \rangle_c = P_1$. It is assumed that the dependence of the dissociation constant on the activity is such that $K_1 > K_0$, i.e., the free energy barrier for binding a ligand to an inactive receptor is smaller. Hence, from Eq. (2) the average activity is a decreasing function of the concentration. This single receptor MWC model already contains the key feature of self-regulation. However, in order to have cooperativity, which is another important feature of the MWC model, we need more than one binding site [8]. The generalization of the model to an arbitrary number of binding sites is contained in Appendix A. For our present purposes it is more convenient to restrict to a single binding site in the main text.

We now consider a nonequilibrium model that includes ATP hydrolysis. For simplicity we assume that when the receptor is unbound only phosphorylation takes place and when the receptor is bound only dephosphorylation occurs. A more general model with phosphorylation and dephosphorylation occurring for both bound and

unbound states, and the implications of this generalization are discussed in section 5. The phosphorylation reaction is represented as



where κ_+^0 and κ_-^0 denote transition rates. The dephosphorylation reaction reads



where ω_+^1 and ω_-^1 are transition rates.

With the free energy (1), the generalized detailed balance relation [33] imposes the following constraints on the rates. First, we have

$$\ln \frac{\kappa_+^0 \omega_+^1}{\kappa_-^0 \omega_-^1} = \Delta\mu + \ln \frac{K_1}{K_0}, \quad (6)$$

where $\Delta\mu = \mu_{\text{ATP}} - \mu_{\text{ADP}} - \mu_{\text{P}_i}$ is the free energy dissipated in one ATP hydrolysis. Second, the transition rates from $b = 0$ to $b = 1$, denoted by w_{01}^a , and from $b = 1$ to $b = 0$, denoted w_{10}^a , fulfill the relation

$$\ln \frac{w_{01}^a}{w_{10}^a} = \ln(c/K_a). \quad (7)$$

With these two constraints the product of the transition rates in a cycle in the clockwise direction in Fig. 1 is precisely $\Delta\mu$, which is the affinity driving the process out of equilibrium. For simplicity we use the specific transition rates given in Fig. 1. The parameters γ_a and γ_b set the time-scale of the active/inactive and bound/unbound transitions, respectively. The parameter α is related to redistributing energy weights among the transition rates in such way that the constraints (6) and (7) are still fulfilled.

A reasonable assumption is that ligand binding is much faster than activity changes, i.e., $\gamma_a/\gamma_b \ll 1$ [3]. With this assumption, calculating the stationary probability distribution using standard methods [34, 35] we obtain

$$\frac{P_0}{P_1} = e^{\Delta E - \Delta\mu} \left(\frac{1 + \frac{c}{K_0}}{1 + \frac{c}{K_1}} \right) \left(\frac{1 + \alpha \frac{c}{K_0}}{1 + \alpha \frac{c}{K_0} e^{-\Delta\mu}} \right). \quad (8)$$

Comparing with the equilibrium expression (8) there is the extra term of the second brackets, which becomes 1 for $\Delta\mu = 0$. The precise effect of this extra term in sensing is discussed in the next section. For this discussion it is convenient to define the effective dissociation constants

$$\tilde{K}_0 \equiv \frac{K_0}{\alpha} \quad \text{and} \quad \tilde{K}_1 \equiv \frac{K_0}{\alpha} e^{\Delta\mu}. \quad (9)$$

3. Integrated sensitivity

A key observable in sensing is the sensitivity

$$R(c, \Delta E) \equiv -4 \frac{\partial}{\partial \ln c} \langle a \rangle_c = -4 \frac{\partial P_1}{\partial \ln c}, \quad (10)$$

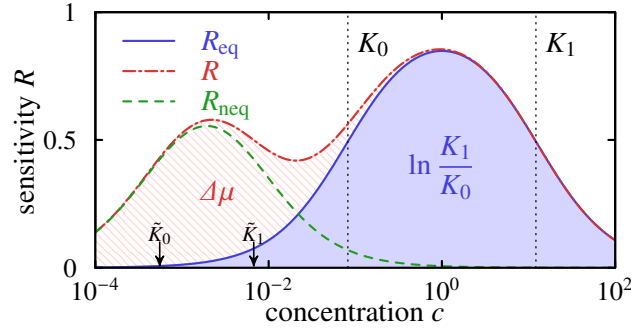


Figure 2. Increase in sensitivity $R(c)$ through nonequilibrium driving. The full blue region under the curve corresponds to the equilibrium contribution $\ln(K_1/K_0)$, while the striped region highlights the additional nonequilibrium enhancement, which is equal to the driving affinity $\Delta\mu$. The parameters are set to $K_1 = 1/K_0 = e^{2.5}$, $\alpha = e^5$, and $\Delta\mu = 2.5$.

which is the response of the average activity to small changes in ligand concentration. It is convenient to rewrite the sensitivity as

$$R(c, \Delta E) = 4P_0P_1 \frac{\partial}{\partial \ln c} \ln \frac{P_0}{P_1} \leq \frac{\partial}{\partial \ln c} \ln \frac{P_0}{P_1}, \quad (11)$$

where the inequality comes from $P_0P_1 \leq 1/4$. From Eq. (8) it follows that the upper bound on the right hand side of Eq. (11) does not depend on ΔE . Hence, for given c there is an optimal conformational free energy difference that maximizes the sensitivity

$$\Delta E^*(c) = \Delta\mu + \ln \left(\frac{1 + \frac{c}{K_1}}{1 + \frac{c}{K_0}} \right) + \ln \left(\frac{1 + \alpha \frac{c}{K_0} e^{-\Delta\mu}}{1 + \alpha \frac{c}{K_0}} \right), \quad (12)$$

which is obtained from Eq. (8) with $P_0P_1 = 1/4$. A free energy close to this optimal value can be achieved through an adaptation system that uses the methylation levels to adjust ΔE in accordance with the external concentration [13]. From now on we set $\Delta E = \Delta E^*(c)$ and denote this maximal sensitivity by $R(c) \equiv R(c, \Delta E^*(c))$.

For the equilibrium case, expressed in Eq. (2), the sensitivity becomes

$$R_{\text{eq}}(c) = \frac{c}{c + K_0} - \frac{c}{c + K_1}. \quad (13)$$

Whereas out of equilibrium, with the ratio of probabilities in Eq. (8), we obtain

$$R(c) = R_{\text{eq}}(c) + R_{\text{neq}}(c), \quad (14)$$

with

$$R_{\text{neq}}(c) = \frac{c}{c + \left(\frac{K_0}{\alpha}\right)} - \frac{c}{c + \left(\frac{K_0 e^{\Delta\mu}}{\alpha}\right)} = \frac{c}{c + \tilde{K}_0} - \frac{c}{c + \tilde{K}_1}. \quad (15)$$

Therefore, the effect of adding a driving affinity $\Delta\mu$ to the single receptor is to increase the sensitivity by $R_{\text{neq}}(c)$. Particularly, the sensitivity of this single receptor out of equilibrium is equal to the sensitivity of a equilibrium model that has a second binding site with dissociation constant \tilde{K}_a , as given by (9). This situation is represented in

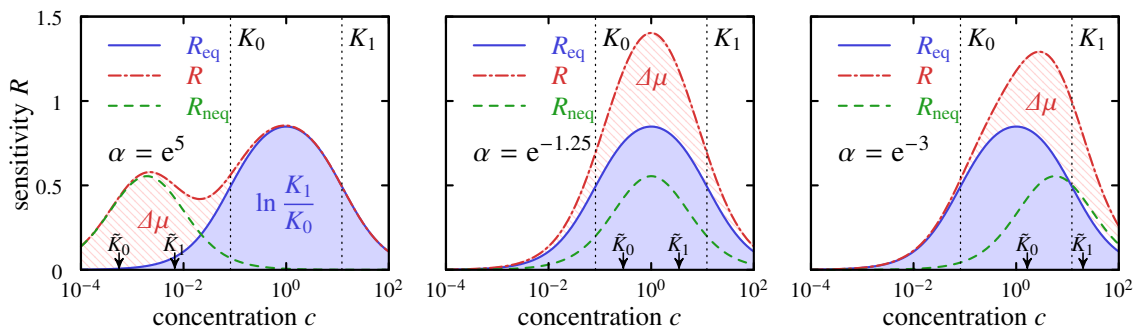


Figure 3. Effect of parameter α on the sensitivity $R(c)$. The parameter α is indicated in the figures, $K_1 = 1/K_0 = e^{2.5}$, and $\Delta\mu = 2.5$. For $\alpha = e^5$ the driving affinity increases the range for which the sensitivity is non-negligible, while in the other two cases we can see a clear increase in the sensitivity in the equilibrium range $K_0 \leq c \leq K_1$, with $\alpha = e^{1.25}$ corresponding to the optimal increase in the equilibrium range.

Fig. 2, where we show the equilibrium contribution to sensitivity peaking between the concentration range $K_0 \leq c \leq K_1$ and the nonequilibrium contribution peaking between the range $\tilde{K}_0 \leq c \leq \tilde{K}_1$. Calculating the maximum of $R_{\text{neq}}(c)$, with c as the optimizing parameter, we obtain the inequality

$$R_{\text{neq}}(c) \leq \frac{e^{\Delta\mu/2} - 1}{e^{\Delta\mu/2} + 1}. \quad (16)$$

We note that an enhancement on sensitivity due to a nonequilibrium driving affinity has been shown in [9] (see also [10]).

As a first main result, we obtain that the integrated sensitivity I has the following simple relation with the driving affinity $\Delta\mu$,

$$I \equiv \int_{-\infty}^{\infty} d(\ln c) R(c) = \Delta\mu + \ln \frac{K_1}{K_0}, \quad (17)$$

where we used Eqs. (13), (14) and (15). This result for the integrated sensitivity provides a precise quantification of the effect of free energy dissipation on sensing. The integral represents the area under the curves in Fig. 2 where the equilibrium contribution $R_{\text{eq}}(c)$ yields $\ln(K_1/K_0)$ and the nonequilibrium contribution rises the area under the curve by $\Delta\mu$.

From the expressions (13) and (15) it follows that $R_{\text{eq}}(c) \leq 1$ and $R_{\text{neq}}(c) \leq 1$, respectively. The effect of the driving affinity on the sensitivity is twofold: it can increase the concentration range for which the sensitivity is non-negligible and it can increase the sensitivity in the equilibrium range $K_0 \leq c \leq K_1$. The nonequilibrium enhancement can even lead to $R(c) > 1$ within this region.

The influence of the parameter α as determined by Eq. (15) on these two effects is shown in Fig. 3, which indicates that there is an optimal α for which the effect of $\Delta\mu$ is mostly to increase the sensitivity in the equilibrium range $K_0 \leq c \leq K_1$. To quantify

the enhancement of sensitivity in this equilibrium range we define the integral

$$\begin{aligned} I_{K_0, K_1}^{\text{neq}} &\equiv \int_{\ln K_0}^{\ln K_1} d(\ln c) R_{\text{neq}}(c) \\ &= \ln \left(\frac{K_1 + \frac{K_0}{\alpha}}{K_1 + \frac{K_0}{\alpha} e^{\Delta\mu}} \right) - \ln \left(\frac{K_0 + \frac{K_0}{\alpha}}{K_0 + \frac{K_0}{\alpha} e^{\Delta\mu}} \right), \end{aligned} \quad (18)$$

We point out that $I_{K_0, K_1}^{\text{neq}} \leq \Delta\mu$ due to Eq. (17) and $I_{K_0, K_1}^{\text{neq}} \leq \ln(K_1/K_0)$ due to $R_{\text{neq}}(c) \leq 1$. Maximizing this integral with respect to α we obtain

$$I_{K_0, K_1}^{\text{neq, opt}} \equiv \max_{\alpha} I_{K_0, K_1}^{\text{neq}} = \ln \left[\frac{K_1}{K_0} \left(\frac{e^{\Delta\mu/2} + \sqrt{\frac{K_0}{K_1}}}{e^{\Delta\mu/2} + \sqrt{\frac{K_1}{K_0}}} \right)^2 \right], \quad (19)$$

where the maximum is obtained for $\alpha = \sqrt{K_0/K_1} \exp(\Delta\mu/2)$, which leads to dissociation constants that satisfy $\tilde{K}_0 \tilde{K}_1 = K_0 K_1$. Hence, expression (19) provides the optimal sensitivity enhancement due to the driving affinity $\Delta\mu$ within the equilibrium concentration range $K_0 \leq c \leq K_1$ for given $\Delta\mu$, K_0 , and K_1 . We note that the effect of increasing the sensitivity beyond the equilibrium range can represent an important advantage for the cell. This increase is quantified by $I - \ln(K_1/K_0) - I_{K_0, K_1}^{\text{neq}}$. A more quantitative relation could arise from studying the sensitivity integrated over some concentration range of interest. Our choice in Eq. (18) is motivated by the fact that $I_{K_0, K_1}^{\text{neq}}$ is convenient for the analogy between nonequilibrium sensing and kinetic proofreading.

4. Analogy with kinetic proofreading

In this section we establish an explicit analogy between sensing with nonequilibrium receptors and kinetic proofreading, with the integrated sensitivity in Eq. (18) playing the role of the error reduction due to dissipation in kinetic proofreading.

4.1. Kinetic proofreading

The model for kinetic proofreading is illustrated in Fig 4. Two substrates $S = R, W$, with R being the ‘‘right’’ substrate and W the ‘‘wrong’’ substrate, can bind to the enzyme E. In equilibrium, the substrate R is copied to a template with higher probability due to a free energy difference ΔF . Specifically, this free energy difference between state EW and ER leads to an equilibrium error

$$\epsilon_{\text{eq}} = \exp(-\Delta F), \quad (20)$$

where the error is defined as the ratio between the probability of writing W and the probability of writing R to the template [22, 23].

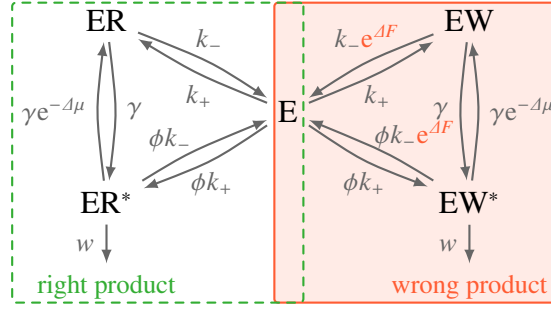


Figure 4. Model for kinetic proofreading. The difference in the transition rates for the two cycles is in the free energy term $e^{\Delta F}$ in the transition from EW to E and from EW* to E, which is related to the higher free energy of EW in comparison to ER. The rate at which information is written w is assumed to be small compared to the other transition rates.

In the kinetic proofreading scheme phosphorylated forms of the substrates are added, leading to the additional states EW* and ER*. The transitions in Fig. 4 involve phosphorylation reactions



and dephosphorylation reactions



If a cycle $\text{E} \rightarrow \text{ES} \rightarrow \text{ES}^* \rightarrow \text{E}$ is completed, one ATP is consumed and $\text{ADP} + \text{P}_i$ is produced, leading to a free energy consumption of $\Delta\mu = \mu_{\text{ATP}} - \mu_{\text{ADP}} - \mu_{\text{P}_i}$. The specific transition rates are shown in Fig. 4, where k_- , k_+ , γ , and ϕ are kinetic parameters. Moreover, w is the rate at which the substrate S is written to the template, which we assume to be much slower than the other transition rates, i.e., we assume the limit $w \rightarrow 0$.

The error is given by

$$\epsilon \equiv \frac{P_{\text{EW}^*}}{P_{\text{ER}^*}} = \left(\frac{(e^{-\Delta\mu} + \phi)\gamma + \phi k_-}{(e^{-\Delta\mu} + \phi)\gamma e^{\Delta F} + \phi k_- e^{2\Delta F}} \right) \left(\frac{(1 + \phi)\gamma + \phi k_- e^{\Delta F}}{(1 + \phi)\gamma + \phi k_-} \right), \quad (23)$$

where P_{EW^*} and P_{ER^*} denote the stationary probabilities of states EW* and ER*, respectively. Hence, as first observed by Hopfield and Ninio [22, 23], with energy dissipation the error can be smaller than ϵ_{eq} . The maximal error reduction $\epsilon/\epsilon_{\text{eq}} = e^{-\Delta F}$ takes place for an appropriate choice of the kinetic parameters and the formal limit $\Delta\mu \rightarrow \infty$.

4.2. Non-equilibrium sensing vs. kinetic proofreading

The minimal error ϵ_{opt} for fixed free energy difference ΔF and driving affinity $\Delta\mu$, that is obtained by optimizing ϵ in Eq. 23 with respect to the kinetic parameters, is given

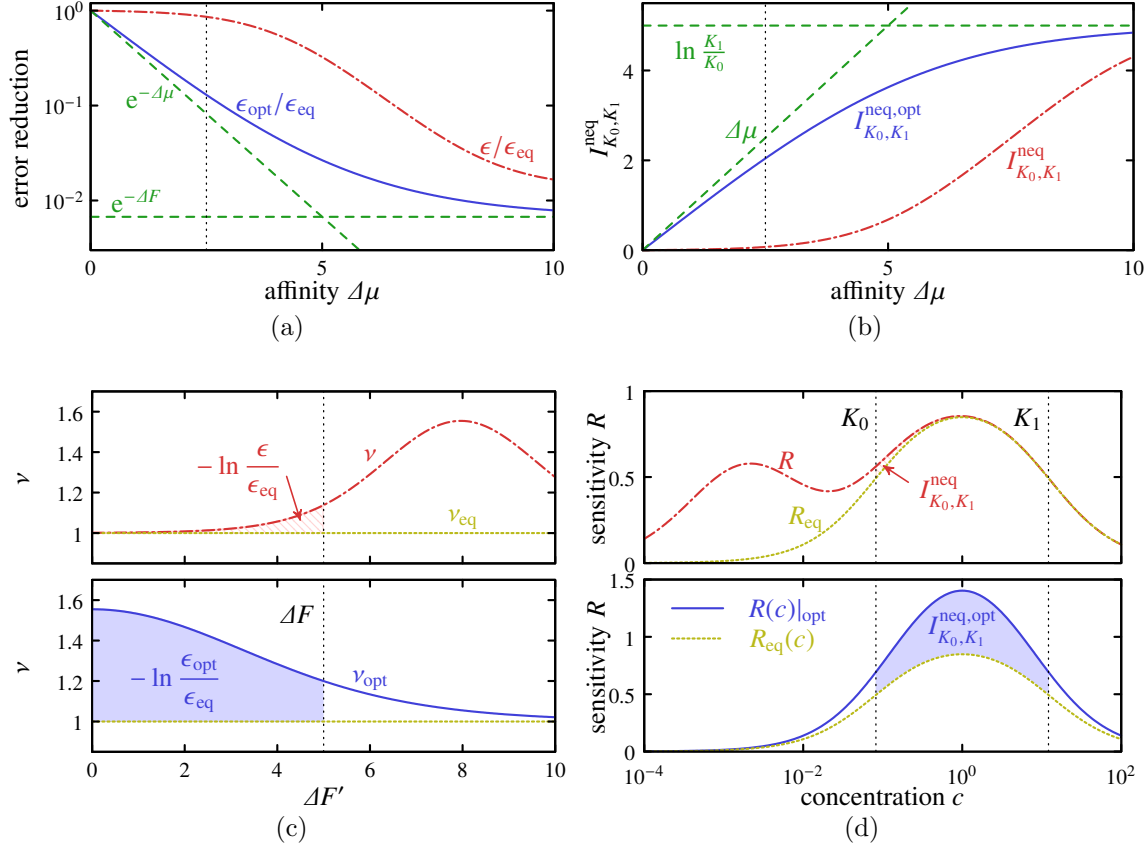


Figure 5. Kinetic proofreading (left panel) versus nonequilibrium sensing (right panel). **(a)** Error reduction $\epsilon/\epsilon_{\text{eq}}$ and optimal error reduction $\epsilon_{\text{opt}}/\epsilon_{\text{eq}}$, as given by (24), as functions of the affinity $\Delta\mu$. The green dashed lines indicate the asymptotically reached bounds $\epsilon_{\text{opt}}/\epsilon_{\text{eq}} \geq e^{-\Delta\mu}$ and $\epsilon_{\text{opt}}/\epsilon_{\text{eq}} \geq e^{-\Delta F}$. **(b)** Nonequilibrium contribution to the sensitivity integrated in the equilibrium range $I_{K_0, K_1}^{\text{neq}}$ and its optimized value $I_{K_0, K_1}^{\text{neq, opt}}$, as given by (19), as functions of the affinity $\Delta\mu$. The green dashed lines indicate the asymptotically reached bounds $I_{K_0, K_1}^{\text{neq}} \leq \Delta\mu$ and $I_{K_0, K_1}^{\text{neq}} \leq \ln(K_1/K_0)$. **(c)** The discriminatory index ν as a function of the free energy difference $\Delta F'$. The lower panel shows $\nu_{\text{opt}} \equiv -\partial_{\Delta F} \ln \epsilon_{\text{opt}}(\Delta F, \Delta\mu)$, i.e., the discriminatory index associated with the minimal error (24). The highlighted areas illustrate relation (27). **(d)** The sensitivity $R(c)$ and the sensitivity $R(c)|_{\text{opt}}$, which is associated with $I_{K_0, K_1}^{\text{neq, opt}}$. The highlighted areas illustrate relation (18). Parameters are set in the following way: $\Delta F = \ln(K_1/K_0) = 5$ with $K_1 = 1/K_0$ in (a) and (b); $\Delta\mu = 2.5$ in (c) and (d); in (b) and (d) $I_{K_0, K_1}^{\text{neq}}$ is obtained from (18) with $\alpha = e^5$; in (a) and (c) $\epsilon/\epsilon_{\text{eq}}$ is obtained from (23) with $k_- = \gamma = 1$, $\phi = 10^{-4}$. The dotted vertical line in (a) and (b) indicate the affinity $\Delta\mu = 2.5$. The dotted vertical line in (c) indicates $\Delta F = 5$.

by [26, 27]

$$\frac{\epsilon_{\text{opt}}}{\epsilon_{\text{eq}}}(\Delta F, \Delta\mu) = e^{-\Delta F} \left(\frac{e^{\frac{\Delta\mu}{2}} + e^{\frac{\Delta F}{2}}}{e^{\frac{\Delta\mu}{2}} + e^{-\frac{\Delta F}{2}}} \right)^2, \quad (24)$$

Since this function is bounded by $e^{-\Delta\mu}$ and by $e^{-\Delta F}$, the following inequality holds [26],

$$\epsilon \geq \epsilon_{\text{opt}} \geq \exp(-\Delta F - \Delta\mu). \quad (25)$$

Comparing expression (24) for the maximal error reduction in kinetic proofreading with expression (19) for the maximal increase in the integrated sensitivity in nonequilibrium sensing, a quite transparent analogy arises, as shown in Figs. 5a and 5b. Both expressions are the same with the increase in sensitivity in the equilibrium range $I_{K_0, K_1}^{\text{neq, opt}}$ being analogous to $-\ln(\epsilon_{\text{opt}}/\epsilon_{\text{eq}})$ and the ratio of the dissociation constants K_1/K_0 being analogous to $e^{\Delta F}$. Whereas in kinetic proofreading a driving affinity $\Delta\mu$ decreases the error, in nonequilibrium sensing $\Delta\mu$ increases the integrated sensitivity in the equilibrium range $K_0 \leq c \leq K_1$.

A recently introduced quantity in kinetic proofreading is the discriminatory index [32]

$$\nu(\Delta F) \equiv -\frac{\partial}{\partial \Delta F} \ln \epsilon, \quad (26)$$

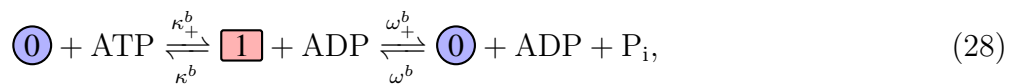
where ϵ is given by (23). Due to $\epsilon_{\text{eq}} = e^{-\Delta F}$ the discriminatory index is $\nu_{\text{eq}} = 1$ in equilibrium, with a larger index $\nu \geq 1$ requiring energy dissipation. We can rewrite (26) as

$$-\ln \frac{\epsilon}{\epsilon_{\text{eq}}} = \int_0^{\Delta F} d\Delta F' [\nu(\Delta F') - 1]. \quad (27)$$

Comparing this equation with (18) we observe that the discriminatory index is analogous to the sensitivity $R(c)$, with $\nu(\Delta F') - 1$ being the nonequilibrium contribution. In Figs. 5c and 5d we show the comparison between discriminatory index in proofreading and sensitivity in nonequilibrium sensing. Murugan et al. [32] have shown that the integral from $-\infty$ to ∞ of $\nu(\Delta F) - 1$ can be equal to $\Delta\mu$. This result is equivalent to our equality (17).

5. Effect of the occupancy of the receptor on phosphorylation and dephosphorylation rates

We now generalize the model from Fig. 1 to include phosphorylation and dephosphorylation reactions for both $b = 0$ and $b = 1$. With this generalization there are two links for the vertical transitions in Fig. 6a. These reactions happen with transition rates



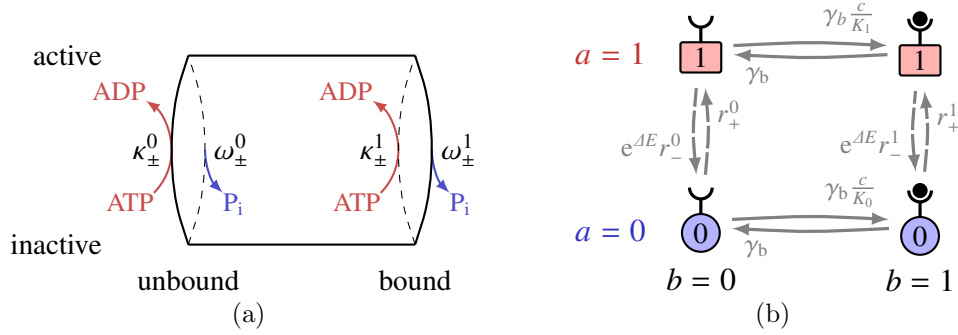


Figure 6. Four-state system with phosphorylation and dephosphorylation for both $b = 0$ and $b = 1$. **(a)** Full model with two links for the vertical transitions. The dashed links indicate transition rates that are zero in the model of Fig. 1. **(b)** Total rates as given by (32) and (33). The coarse-grained entropy production (43) is calculated with these total transition rates.

where $b = 0, 1$. For thermodynamic consistency, the following constraints must be fulfilled:

$$\Delta\mu = \ln \frac{\kappa_+^b \omega_+^b}{\kappa_-^b \omega_-^b} \quad (29)$$

for $b = 0, 1$,

$$\ln \frac{\kappa_+^0 \omega_+^1}{\kappa_-^0 \omega_-^1} = \Delta\mu + \ln \frac{K_1}{K_0}, \quad (30)$$

and

$$\ln \frac{\kappa_+^1 \omega_+^0}{\kappa_-^1 \omega_-^0} = \Delta\mu - \ln \frac{K_1}{K_0}, \quad (31)$$

where we used the free energy (1) for the second and third equations. Whereas the presence of two links is important for calculating the rate of dissipation in this model [33], for the purpose of calculating the stationary probabilities we consider the total transition rates from inactive to active

$$r_+^b \equiv \kappa_+^b + \omega_-^b \quad (32)$$

and from active to inactive

$$e^{\Delta E} r_-^b \equiv \kappa_-^b + \omega_+^b, \quad (33)$$

which are indicated in Fig. 6b. We choose the rates κ_-^b and ω_+^b to be proportional to $e^{\Delta E}$, which leads to r_-^b independent of ΔE . Assuming that the binding/unbinding transitions are much faster, the ratio of stationary probabilities (8) for this more general model becomes

$$\frac{P_0}{P_1} = e^{\Delta E} \left(\frac{1 + \frac{c}{K_0}}{1 + \frac{c}{K_1}} \right) \left(\frac{r_-^0 + (\frac{c}{K_1})r_-^1}{r_+^0 + (\frac{c}{K_0})r_+^1} \right) \equiv e^{\Delta E} \left(\frac{1 + \frac{c}{K_0}}{1 + \frac{c}{K_1}} \right) \chi(c). \quad (34)$$

As in section 3, the sensitivity (11) is maximized for $P_0/P_1 = 1$, which is achieved at

$$\Delta E^*(c) = \ln \left(\frac{1 + \frac{c}{K_1}}{1 + \frac{c}{K_0}} \right) - \ln \chi(c), \quad (35)$$

The equilibrium contribution to the maximal sensitivity is given by (13), while the nonequilibrium contribution is

$$R_{\text{neq}}(c) \equiv \frac{\partial}{\partial(\ln c)} \ln \chi(c) = \frac{1}{c} \frac{\chi'(c)}{\chi(c)}. \quad (36)$$

The integrated sensitivity then becomes

$$\begin{aligned} I &= \int_{-\infty}^{\infty} d(\ln c) [R_{\text{neq}}(c) + R_{\text{eq}}(c)] = \ln \frac{K_1}{K_0} + \ln \frac{\chi(\infty)}{\chi(0)} \\ &= \ln \left(\frac{r_+^0 r_-^1}{r_-^0 r_+^1} \right). \end{aligned} \quad (37)$$

For $\Delta\mu \geq 0$, from Eqs. (29), (32), and (33), we obtain

$$\frac{\omega_-^b}{\omega_+^b} \leq \frac{r_+^b}{e^{\Delta E} r_-^b} \leq \frac{\kappa_+^b}{\kappa_-^b}. \quad (38)$$

With these inequalities, we obtain that the integrated sensitivity (37) is bounded by

$$I = \ln \left(\frac{r_+^0 r_-^1}{r_-^0 r_+^1} \right) \leq \ln \frac{\kappa_+^0 \omega_+^1}{\kappa_-^0 \omega_-^1} = \ln \frac{K_1}{K_0} + \Delta\mu, \quad (39)$$

where we used (30) in the last equality. As shown in Appendix A, this inequality can also be generalized to an arbitrary number of binding sites.

The influence of how the occupancy of the receptor affects the reaction rates for activity on the relation between the integrated sensitivity I and the driving affinity $\Delta\mu$ can be seen with the following examples. First, if we choose transition rates satisfying the relation

$$\frac{K_0 r_-^1}{K_1 r_+^1} = \frac{r_-^0}{r_+^0}, \quad (40)$$

the function $\chi(c)$ in (34) becomes independent of c . In this case, from (36) we obtain $R_{\text{neq}}(c) = 0$, which implies $I = \ln(K_1/K_0)$. Hence, it is possible to have a dissipative model with ATP consumption that has the same sensitivity as the equilibrium case. Second, we consider the case where phosphorylation happens only if the receptor is bound and dephosphorylation occurs only if the receptor is unbound, which is the opposite of the model in Fig. 1. In this case $\kappa_{\pm}^0 = \omega_{\pm}^1 = 0$, leading to

$$I = \ln \frac{\kappa_-^1 \omega_-^0}{\kappa_+^1 \omega_+^0} = \ln \frac{K_1}{K_0} - \Delta\mu, \quad (41)$$

where we used (39) and (31). This result shows that the integrated sensitivity can also decrease with energy dissipation. The regime for which the integrated sensitivity is decreased by $\Delta\mu$ is equivalent to an anti-proofreading regime recently studied in [32].

A more precise analysis of the relation between I and energy dissipation can be achieved by considering the entropy production σ [33]. For the present model this entropy production is the rate of ATP consumption. Using the stationary probability $P_{a,b}$ we define the probability current $J_b \equiv P_{0,b}\kappa_+^b - P_{1,b}\kappa_-^b$. With this current the entropy production can be written as

$$\sigma = (J_0 + J_1)\Delta\mu, \quad (42)$$

by using the fact that σ is a sum of currents multiplying cycle affinities [33]. The energy dissipation σ is non-zero whenever $\Delta\mu \neq 0$. Besides σ , we can consider a coarse-grained entropy production $\tilde{\sigma}$, which does not take into account the two channels for the vertical transitions in Fig. 6a: it is obtained by considering the single links with rates r_{\pm}^b in Fig. 6b. This coarse-grained entropy production provides a lower bound on the full entropy production, i.e., $\sigma \geq \tilde{\sigma}$ [36]. For the model in Fig. 6b,

$$\tilde{\sigma} = J\mathcal{A}. \quad (43)$$

where $J \equiv r_+^0 P_{0,0} - e^{\Delta E} r_-^0 P_{1,0}$ and

$$\mathcal{A} \equiv \ln \left(\frac{r_+^0 r_-^1}{r_-^0 r_+^1} \right) - \ln \frac{K_1}{K_0} \quad (44)$$

is an effective affinity. From relation (39) we obtain

$$\mathcal{A} = I - \ln \frac{K_1}{K_0}, \quad (45)$$

which is the nonequilibrium contribution to the integrated sensitivity I . The effective affinity associated with the coarse-grained entropy production determines three different regimes for nonequilibrium sensing. For $\mathcal{A} > 0$ the integrated sensitivity is increased in relation to its equilibrium value. If $\mathcal{A} = 0$, which implies $\tilde{\sigma} = 0$, the energy dissipation has no effect on sensitivity. If $\mathcal{A} < 0$ then the inequality $\tilde{\sigma} \geq 0$ implies $J < 0$. In this last regime energy dissipation decreases the integrated sensitivity.

6. Conclusion

We have characterized the enhancement of sensitivity by a nonequilibrium driving affinity that arises from ATP hydrolysis in the chemical reactions involving an activity change. For the single receptor model from Sec. 2, the integrated sensitivity I was shown to have a simple relation with the driving affinity in Eq. (17). We have shown that a dissipative sensing model can lead to both an increase in the concentration range for which the sensitivity is non-negligible and an increase in the sensitivity in the equilibrium range. The second effect is quantified by $I_{K_0, K_1}^{\text{neq}}$, which is defined in Eq. (18).

We have shown that nonequilibrium sensing is equivalent to kinetic proofreading, with the analogous parameters, observables and relations summarized in Tab. 1. Most prominently, while in nonequilibrium sensing a driving affinity leads to an increase in the sensitivity integrated over the equilibrium range, in kinetic proofreading a driving

Nonequilibrium sensing	$I_{K_0K_1}^{\text{neq}}$	R	$\ln(K_1/K_0)$	$I \leq \ln(K_1/K_0) + \Delta\mu$
Kinetic proofreading	$-\ln(\epsilon/\epsilon_{\text{eq}})$	ν	ΔF	$\epsilon \geq \exp(-\Delta F - \Delta\mu)$

Table 1. Nonequilibrium sensing compared to kinetic proofreading.

affinity decreases the error. In kinetic proofreading the equivalent of sensitivity is the discriminatory index introduced in [32].

The influence of the occupancy of the receptor on the phosphorylation and dephosphorylation rates is of fundamental importance for the relation between integrated sensitivity and the affinity. As we have shown in section 5, it is even possible to have a regime where energy dissipation leads to a decrease on the integrated sensitivity, which is analogous to the anti-proofreading regime from [32].

Our results demonstrate that measurements of the integrated sensitivity could unveil how the occupancy of the receptor affects the phosphorylation and dephosphorylation rates. It is certainly intriguing to speculate whether real chemotaxis networks evolved in such a way that this influence optimizes the enhancement of sensitivity due to energy consumption.

Acknowledgments

D. H. acknowledges helpful discussions with J. M. Sánchez.

Appendix A. Generalization to an arbitrary number of binding sites

In this Appendix, we consider a generalization of the model studied in the main text for an arbitrary number of binding sites. In this case, the variable b takes the values $b = 0, 1, \dots, N$, where N the number of binding sites. The transition rates for this more general model are shown in Fig. A1. Rates involving a change in activity are given by (32) and (33). Rates related to a change in the occupancy of receptor must fulfill the generalized detailed balance relation with respect to the free energy (1). We set these rates as follows. The binding rate from b to $b + 1$ is $w_{b,b+1}^a = \gamma_b(N - b)c/K_a$, where the factor $N - b$ comes from the fact that there are $N - b$ free receptors for the ligand to bind; the unbinding rate from b to $b - 1$ is $w_{b,b-1}^a = \gamma_b b$, where the factor b is related to the number of bound receptors.

We assume that the binding events are much faster than changes in activity. In this case, the stationary conditional probability reads

$$P(b|a) \equiv \frac{P_{a,b}}{P_a} = \binom{N}{b} \left(\frac{c}{K_a}\right)^b \bigg/ \left(1 + \frac{c}{K_a}\right)^N, \quad (\text{A.1})$$

leading to

$$\frac{P_0}{P_1} = e^{\Delta E} \left(\frac{1 + \frac{c}{K_0}}{1 + \frac{c}{K_1}}\right)^N \chi(c), \quad (\text{A.2})$$

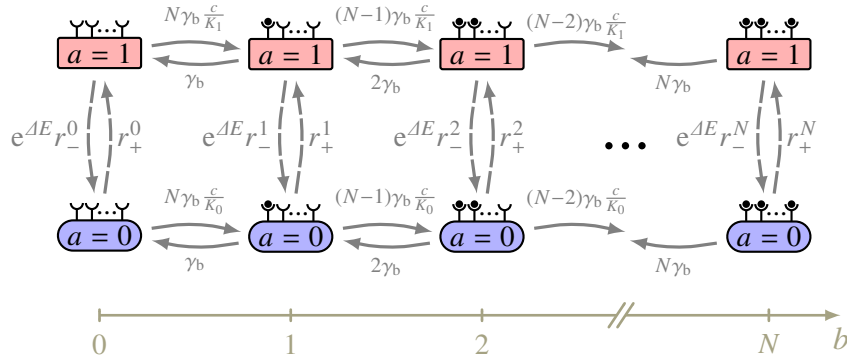


Figure A1. Generalization of the single receptor model in the main text to an arbitrary number of binding sites N . The rates r_+^b and $e^{\Delta E} r_-^b$ are defined in (32) and (33), respectively.

where

$$\chi(c) = \frac{\sum_{b=0}^N \binom{N}{b} \left(\frac{c}{K_1}\right)^b r_-^b}{\sum_{b=0}^N \binom{N}{b} \left(\frac{c}{K_0}\right)^b r_+^b}. \quad (\text{A.3})$$

This expression generalizes (34) to the case of N binding sites. Following the same procedure from section 5, similarly to (35) the sensitivity (11) is maximized for

$$\Delta E^*(c) = N \ln \left(\frac{1 + \frac{c}{K_1}}{1 + \frac{c}{K_0}} \right) - \ln \chi(c), \quad (\text{A.4})$$

where, similarly to (36), the nonequilibrium contribution to sensitivity becomes

$$R_{\text{neq}}(c) = \frac{\partial}{\partial(\ln c)} \ln \chi(c) = \frac{1}{c} \frac{\chi'(c)}{\chi(c)}. \quad (\text{A.5})$$

Hence, the integrated sensitivity reads

$$\begin{aligned} I &= \int_{-\infty}^{\infty} d(\ln c) [R_{\text{eq}}(c) + R_{\text{neq}}(c)] = N \ln \frac{K_1}{K_0} + \ln \frac{\chi(\infty)}{\chi(0)} \\ &= \ln \left(\frac{r_+^0 r_-^N}{r_-^0 r_+^N} \right). \end{aligned} \quad (\text{A.6})$$

The transition rates for this model must fulfill the constraint

$$\ln \left(\frac{\kappa_+^0 \omega_+^N}{\kappa_-^0 \omega_-^N} \right) = N \ln \frac{K_1}{K_0} + \Delta\mu. \quad (\text{A.7})$$

From the inequalities (38) we finally obtain

$$I \leq N \ln \frac{K_1}{K_0} + \Delta\mu, \quad (\text{A.8})$$

which generalizes inequality (39) to the case of N binding sites.

References

- [1] H. C. Berg and D. A. Brown, “Chemotaxis in escherichia coli analysed by three-dimensional tracking,” *Nature* **239** (1972) 500–504.
- [2] H. C. Berg, *E. coli in Motion*. Springer, New York, 2004.
- [3] Y. Tu, T. S. Shimizu, and H. C. Berg, “Modeling the chemotactic response of escherichia coli to time-varying stimuli,” *Proc. Natl. Acad. Sci. USA* **105** (2008) 14855–60.
- [4] B. A. Mello and Y. Tu, “Effects of adaptation in maintaining high sensitivity over a wide range of backgrounds for escherichia coli chemotaxis,” *Biophys. J.* **92** (2007) 2329–37.
- [5] Y. Tu, “Quantitative modeling of bacterial chemotaxis: Signal amplification and accurate adaptation,” *Ann. Rev. Biophys.* **42** (2013) 337–359.
- [6] D. Clausznitzer, G. Micali, S. Neumann, V. Sourjik, and R. G. Endres, “Predicting chemical environments of bacteria from receptor signaling,” *PLoS Comput. Biol.* **10** (2014) e1003870.
- [7] J. Monod, J. Wyman, and J.-P. Changeux, “On the nature of allosteric transitions: A plausible model,” *J. Mol. Biol.* **12** (1965) 88–118.
- [8] S. Marzen, H. G. Garcia, and R. Phillips, “Statistical mechanics of Monod–Wyman–Changeux (MWC) models,” *J. Mol. Biol.* **425** (2013) 1433–60.
- [9] Y. Tu, “The nonequilibrium mechanism for ultrasensitivity in a biological switch: Sensing by maxwell’s demons,” *Proc. Natl. Acad. Sci. USA* **105** (2008) 11737–41.
- [10] M. Skoge, S. Naqvi, Y. Meir, and N. S. Wingreen, “Chemical sensing by nonequilibrium cooperative receptors,” *Phys. Rev. Lett.* **110** (2013) 248102.
- [11] H. Qian and T. C. Reluga, “Nonequilibrium thermodynamics and nonlinear kinetics in a cellular signaling switch,” *Phys. Rev. Lett.* **94** (2005) 028101.
- [12] P. Mehta and D. J. Schwab, “Energetic costs of cellular computation,” *Proc. Natl. Acad. Sci. USA* **109** (2012) 17978–82.
- [13] G. Lan, P. Sartori, S. Neumann, V. Sourjik, and Y. Tu, “The energy–speed–accuracy trade-off in sensory adaptation,” *Nature Physics* **8** (2012) 422–428.
- [14] G. De Palo and R. G. Endres, “Unraveling adaptation in eukaryotic pathways: Lessons from protocells,” *PLoS Biol.* **9** (2013) e1003300.
- [15] A. H. Lang, C. K. Fisher, T. Mora, and P. Mehta, “Thermodynamics of statistical inference by cells,” *Phys. Rev. Lett.* **113** (2014) 148103.
- [16] C. C. Govern and P. R. ten Wolde, “Optimal resource allocation in cellular sensing systems,” *Proc. Natl. Acad. Sci. USA* **111** (2014) 17486–91.
- [17] C. C. Govern and P. R. ten Wolde, “Energy dissipation and noise correlations in biochemical sensing,” *Phys. Rev. Lett.* **113** (2014) 258102.
- [18] P. Sartori, L. Granger, C. F. Lee, and J. M. Horowitz, “Thermodynamic costs of information processing in sensory adaptation,” *PLoS Comput. Biol.* **10** (2014) e1003974.
- [19] A. C. Barato, D. Hartich, and U. Seifert, “Information-theoretic versus thermodynamic entropy production in autonomous sensory networks,” *Phys. Rev. E* **87** (2013) 042104.
- [20] A. C. Barato, D. Hartich, and U. Seifert, “Efficiency of cellular information processing,” *New J. Phys.* **16** (2014) 103024.
- [21] S. Bo, M. Del Giudice, and A. Celani, “Thermodynamic limits to information harvesting by sensory systems,” *J. Stat. Mech.* (2015) P01014.
- [22] J. J. Hopfield, “Kinetic proofreading: A new mechanism for reducing errors in biosynthetic processes requiring high specificity,” *Proc. Natl. Acad. Sci. USA* **71** (1974) 4135–39.
- [23] J. Ninio, “Kinetic amplification of enzyme discrimination,” *Biochimie* **57** (1975) 587–595.
- [24] C. H. Bennett, “Dissipation-error tradeoff in proofreading,” *Biosystems* **11** (1979) 85–91.
- [25] M. Ehrenberg and C. Blomberg, “Thermodynamic constraints on kinetic proofreading in biosynthetic pathways,” *Biophys. J.* **31** (1980) 333–358.
- [26] H. Qian, “Reducing intrinsic biochemical noise in cells and its thermodynamic limit,” *J. Mol. Biol.* **362** (2006) 387–392.

- [27] H. Qian, “Phosphorylation energy hypothesis: Open chemical systems and their biological functions,” *Ann. Rev. Phys. Chem.* **58** (2007) 113–142.
- [28] H. Qian, “Cooperativity and specificity in enzyme kinetics: A single-molecule time-based perspective,” *Biophys. J.* **95** (2008) 10–17.
- [29] H. Qian, “Cyclic conformational modification of an enzyme: Serial engagement, energy relay, hysteretic enzyme, and fischer’s hypothesis,” *J. Phys. Chem. B* **114** (2010) 16105–11.
- [30] A. Murugan, D. A. Huse, and S. Leibler, “Speed, dissipation, and error in kinetic proofreading,” *Proc. Natl. Acad. Sci. USA* **109** (2012) 12034–39.
- [31] P. Sartori and S. Pigolotti, “Kinetic versus energetic discrimination in biological copying,” *Phys. Rev. Lett.* **110** (2013) 188101.
- [32] A. Murugan, D. A. Huse, and S. Leibler, “Discriminatory proofreading regimes in nonequilibrium systems,” *Phys. Rev. X* **4** (2014) 021016.
- [33] U. Seifert, “Stochastic thermodynamics, fluctuation theorems and molecular machines,” *Rep. Prog. Phys.* **75** (2012) 126001.
- [34] J. Schnakenberg, “Network theory of microscopic and macroscopic behavior of master equation systems,” *Rev. Mod. Phys.* **48** (1976) 571–585.
- [35] T. L. Hill, *Free Energy Transduction and Biochemical Cycle Kinetics*. Dover Publications, Mineola, New York, 2005.
- [36] M. Esposito, “Stochastic thermodynamics under coarse graining,” *Phys. Rev. E* **85** (2012) 041125.